UC Irvine
UC Irvine Previously Published Works

Title
Highly Charged Particles Cause a Larger Current Blockage in Micropores Compared to Neutral Particles

Permalink
https://escholarship.org/uc/item/9m5709q9

Journal
ACS Nano, 10(9)

ISSN
1936-0851

Authors
Qiu, Yinghua
Lin, Chih-Yuan
Hinkle, Preston
et al.

Publication Date
2016-09-27

DOI
10.1021/acsnano.6b03280

Copyright Information
This work is made available under the terms of a Creative Commons Attribution License, availalbe at https://creativecommons.org/licenses/by/4.0/

Peer reviewed

eScholarship.org Powered by the California Digital Library
University of California

ACSNANO
www.acsnano.org
ARTICLE

Highly Charged Particles Cause a Larger Current Blockage in Micropores Compared to Neutral Particles

Yinghua Qiu,[†,‡,¶] Chih-Yuan Lin,[§,¶] Preston Hinkle,[†] Timothy S. Plett,[†] Crystal Yang,[∥] Jenu Varghese Chacko,[⊥] Michelle A. Digman,[⊥] Li-Hsien Yeh,[*,#] Jyh-Ping Hsu,[*,§] and Zuzanna S. Siwy[*,†,∥,⊥]

[†]Department of Physics and Astronomy, [∥]Department of Chemistry, and [⊥]Department of Biomedical Engineering, University of California, Irvine, California 92697, United States

[‡]School of Mechanical Engineering and Jiangsu Key Laboratory for Design and Manufacture of Micro-Nano Biomedical Instruments, Southeast University, Nanjing 211189, China

[§]Department of Chemical Engineering, National Taiwan University, Taipei 10617, Taiwan

[#]Department of Chemical and Materials Engineering, National Yunlin University of Science and Technology, Yunlin 64002, Taiwan

Supporting Information

ABSTRACT: Single pores in the resistive-pulse technique are used as an analytics tool to detect, size, and characterize physical as well as chemical properties of individual objects such as molecules and particles. Each object passing through a pore causes a transient change of the transmembrane current called a resistive pulse. In high salt concentrations when the pore diameter is significantly larger than the screening Debye length, it is assumed that the particle size and surface charge can be determined independently from the same experiment. In this article we challenge this assumption and show that highly charged hard spheres can cause a significant increase of the resistive-pulse amplitude compared to neutral particles of a similar diameter. As a result, resistive pulses overestimate the size of charged particles by even 20%. The observation is explained by the effect of concentration polarization created across particles in a pore, revealed by numerical modeling of ionic concentrations, ion current, and local electric fields. It is notable that in resistive-pulse experiments with cylindrical pores, concentration polarization was previously shown to influence ionic concentrations only at pore entrances; consequently, additional and transient modulation of resistive pulses was observed when a particle entered or left the pore. Here we postulate that concentration polarization can occur across transported particles at any particle position along the pore axis and affect the magnitude of the entire resistive pulse. Consequently, the recorded resistive pulses of highly charged particles reflect not only the particles' volume but also the size of the depletion zone created in front of the moving particle. Moreover, the modeling identified that the effective surface charge density of particles depended not only on the density of functional groups on the particle but also on the capacitance of the Stern layer. The findings are of crucial importance for sizing particles and characterizing their surface charge properties.

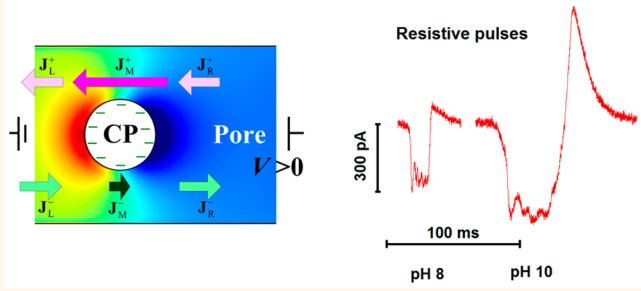

KEYWORDS: *resistive pulse, concentration polarization, particles*

The translocation of a molecule or particle through a pore causes a transient change of the system resistance observed as a transient change of the transmembrane current, called a resistive pulse.[1−9] The amplitude of resistive pulses reflects the object's size; however in some cases it can also be affected by the properties of the background electrolyte. For DNA molecules, when the detection is performed from concentrated KCl solutions, above 0.3 M, the passage of individual strands usually causes a current blockage.[11,12] In contrast, experiments in more diluted electrolyte solutions revealed that the molecules' passage can induce a current increase compared to the baseline current of the empty nanopore.[10,11] The salt concentration dependence of the resistive-pulse amplitude was explained by two competing

Received: May 17, 2016
Accepted: August 17, 2016
Published: August 17, 2016

© 2016 American Chemical Society

DOI: 10.1021/acsnano.6b03280
ACS Nano 2016, 10, 8413−8422

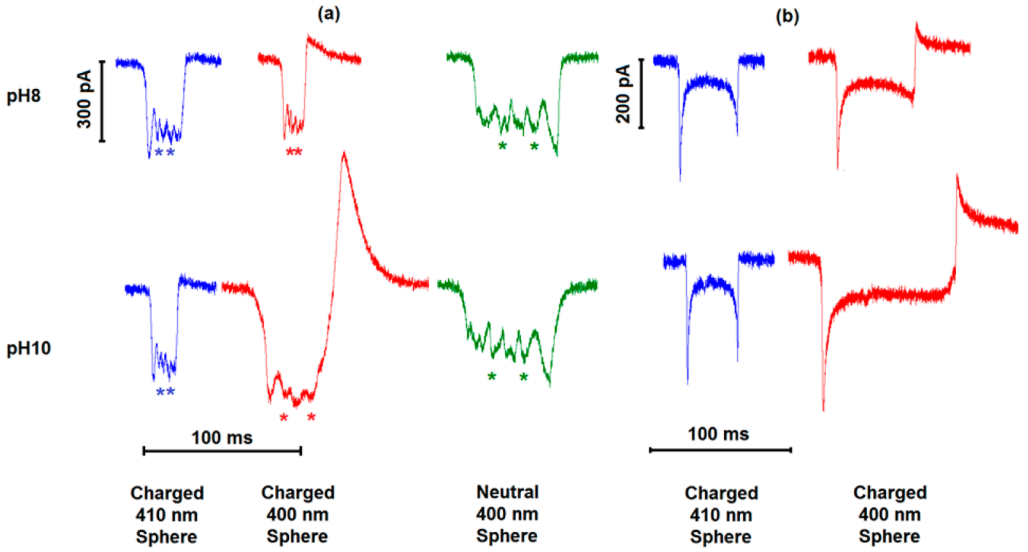

Figure 1. Example passages of three types of polystyrene particles through a single pore in an (a) 11 μm thick PET film (at 0.8 V) and (b) 29 μm thick PC film (at 1.2 V). The PET and PC pores had average opening diameters of 1550 and 1150 nm, respectively. All recordings were performed in 100 mM KCl background electrolyte at pH values as indicated in the figure. Charged 410 nm particles (blue signals) were characterized by 3 times lower density of carboxyl groups compared to the charged 400 nm spheres (red signals). Passage of neutral 400 nm spheres is shown as green traces. Scheme of the experimental setup is shown in Figure S1a. Charged particles moved by electrophoresis toward a positively biased electrode; neutral particles moved by electroosmosis toward a negatively biased electrode (Figure S1b).

effects: (i) volume exclusion and (ii) the presence of additional ions that a charged particle brings to the pore to fulfill electroneutrality. On the basis of these experiments, it is generally assumed that resistive pulses of charged objects are characterized by a lower amplitude compared to neutral particles of the same size.[12] Note that more complex behavior can be observed with conically shaped pores, where the pulse amplitude and shape are also influenced by intrinsic voltage modulations of ionic concentrations.[13−15]

In DNA-detecting experiments, nanopores with openings less than 10 nm are usually used. The surface charges of pore walls and DNA molecules could therefore have a significant effect on the measured current due to the comparable scales of the Debye length and the pore dimension. If resistive-pulse experiments are performed at conditions at which the pore and particle diameters are significantly larger than the Debye screening length, the pulse amplitude was found to be independent of the particle charge. As a result, simultaneous detection of particle size and zeta potential was possible.[16] An exception was provided by mesosized hydrogels passing through meso- and micropores.[17−19] Due to the porosity and low density of the particles, their passage through a pore caused a current increase above the baseline current even in solutions of high ionic strength; the number of counterions the hydrogels brought into the pore was higher than the number of ions excluded by the effective hydrogel's volume.

However, there have been very few studies on the translocation of highly charged hard spheres through pores. Such systems are important due to application of DNA-modified particles in biosensing and nanotechnology.[20,21] Highly charged spheres also present an intriguing physical chemistry system, which exhibits new effects that cannot be described by classical electrostatics. In our recent studies, for example, we showed that translocation velocity of charged polystyrene particles depended in a nontrivial manner on the particle surface charge.[22] Due to ion condensation[23] and nonequilibrium effect of double-layer polarization,[24−26] the passage time of highly charged particles was found to be significantly larger than the passage time of less charged particles. This observation was unexpected, because the methods to measure the surface charge density and zeta potential of particles assume that particles that have more surface charges will move faster.[16]

In this article we show that the dependence of the amplitude of resistive pulses of charged particles can also be unusual and contradict the earlier experiments with DNA.[10,11] Namely, as the surface charge density of polystyrene mesoparticles increased, the amplitude of resistive pulses caused by the particles passing through single micropores was observed to increase as well. The measurements reported here were performed in 0.1 and 0.3 M KCl, thus at conditions at which the Debye length is hundreds of times smaller than the particle's or pore's diameters. The particles' passage occurred electrokinetically, and no pressure difference was applied. The charged particles used in the experiments were carboxylated, and their surface charge density was regulated by the solution pH.[22] The pH dependence of the surface charge was modeled, taking into account the number of surface chemical groups as well as the Stern layer of the particle electrical double layer.[27] The modeling presented here points to the crucial importance of the Stern layer in predicting surface charge density of highly charged particles. The enhanced resistive-pulse amplitude for highly charged particles is explained by (i) modulated ionic concentrations on both sides of a translocating particle and (ii) changed distribution of the local electric fields near the particle, compared to an empty pore. We show that passage of charged particles through pores induces the effect of concentration polarization with a depletion zone formed in front of the passing particle. It is the depletion zone that enhances the current blockage beyond a level expected from the particle volume. In previous studies, concentration polarization in the resistive-pulse experiments with hard spheres was discussed only in the context of modulated ionic concentrations at pore entrances.[13,28] This localized modulation of ionic concen-

DOI: 10.1021/acsnano.6b03280
ACS Nano 2016, 10, 8413−8422

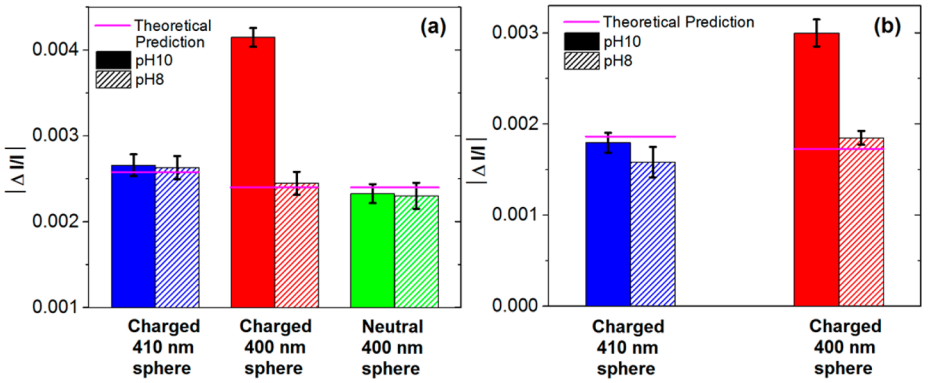

Figure 2. Average current blockage $\Delta I/I$ caused by single particles in single (a) PET (0.8 V) and (b) PC (1.2 V) pores. Recordings from the same pores are shown in Figure 1. The recordings were performed in 100 mM KCl, pH 8 and pH 10. The number of uncharged particles that passed through the PC pore was insufficient to perform detailed statistical analysis. The magenta lines mark the theoretical predictions of $\Delta I/I$ based on the dimensions of particles and pores using equations given in refs 2, 3, and 6

trations was shown to lead to transient changes of the pulse amplitude corresponding to a particle entering and exiting a pore. Note that in short aspect ratio pores, a resistive pulse might be entirely dominated by the entrance effects.[29] This article presents experimental and numerical evidence for the existence of particle-induced concentration polarization at any axial position of a large aspect ratio pore. As a result, resistive pulses of highly charged objects are characterized by significantly higher amplitude compared to pulses of neutral particles of the same diameter. The large aspect ratio pores that are considered here had similar opening diameters at both entrances; thus ionic concentrations in the pore are not dependent on voltage polarity or voltage magnitude in a nonlinear way, as shown before, for example, for conically shaped pores.[13−15]

RESULTS AND DISCUSSION

Resistive-pulse experiments were performed with single track-etched micropores[30] in polyethylene terephthalate (PET)[31,32] and polycarbonate (PC) films.[33] The main difference between pores prepared in the two kinds of polymers is their 3D topography. Due to laminar and semicrystalline structure of the PET films, pores in this material are characterized by large undulations of the local diameter, which are reflected as peaks and valleys in the resistive pulses.[31] A particle blocks the pore to a larger extent when it is passing through a narrower region compared to the blockage caused in a wider zone. Polycarbonate films used in the research are amorphous, and as shown before, track-etched PC pores are smooth along the whole length except the entrances, which feature a smaller diameter.[33,34] Figure 1 shows example passages of three types of ∼400 nm diameter particles through single PET and PC pores; continuous recordings of ion current with resistive pulses are shown in Figure S1. The 410 and 400 nm carboxylated particles differed in the density of surface carboxyl groups by a factor of 3; 410 nm particles were less charged. Neutral polystyrene particles of 400 nm in diameter were also studied. Visual inspection of the recordings (Figures 1, S1, S2) suggests that the pulses created by the highly charged particles are characterized by the largest amplitude and are pH dependent. Note that we were not able to record a statistically significant number of passages of any neutral polystyrene particles through PC pores. This is most probably due to the reduced zeta potential[35] and enhanced hydrophobic properties[36,37] of the PC etched surface compared to PET foils. An example passage of a neutral particle through a PC pore is shown in Figure S2.

In order to analyze the amplitude of the pulses, ΔI, more rigorously, we calculated the average current decrease caused by the particles, as reported before.[33] The analysis was performed by integration of the pulses recorded with the PET pore between points marked with an asterisk in Figure 1a; the pulses for the PC pore were integrated in the flat, constant region (Figure 1b). Figure 2 shows the average relative current blockage obtained in PET and PC single pores in two pH values, pH 8 and 10. Since the two types of studied particles were carboxylated, the increase of pH was expected to lead to the increase of their surface charge density.[38] However, we were surprised to observe that the highly charged particles (400 nm in diameter, red traces in Figure 1) caused a larger current decrease than the weakly charged or uncharged particles (blue and green traces in Figure 1). The difference was especially pronounced at pH 10. This was unexpected, because based on earlier experiments with charged objects, one would predict that the additional counterions the particles bring to the pore should offset some of the volume occlusion.[10−13] The same behavior was observed with smooth polycarbonate pores (Figures 1b, 2b, S2): again the current decrease caused by the highly charged particles at pH 10 was the largest.

As reported before, the exit of negatively and highly charged particles from a pore causes a current increase above the baseline current.[13,28] In the experiments reported here, we again observed a current increase at the end of the pulses corresponding to the highly charged 400 nm particles at pH 10 (Figure 1), further evidencing that increasing pH indeed increases the particle surface charge.[22] The presence of a current increase upon the particle exit made the observation of the increased current blockage with the particle in the pore even more counterintuitive.

In order to quantify the magnitude by which the recordings at pH 10 in 100 mM KCl overestimate the particle size, we used equations relating $\Delta I/I$ with particle and pore diameters.[2,3,6] On the basis of the data shown in Figure 2, we found that the 400 nm charged particles sized as 480 nm in both the PET and PC pores. Figure S3 shows detailed distributions of the particle sizes as determined from the resistive-pulse experiments at pH 8 and pH 10.

The particles' diameter in the two pH conditions was also determined independently using the dynamic light scattering

DOI: 10.1021/acsnano.6b03280
ACS Nano 2016, 10, 8413−8422

approach with a Zetasizer. The highly charged particles in 100 mM KCl (with a nominal diameter of 400 nm as given by the manufacturer) sized as 384 nm at pH 8 and 402 nm at pH 10 (Figure S4). When interpreting these results, we recalled that the dynamic light scattering approach might overestimate the diameter of highly charged particles due to the influence of surface charges on the particles' Brownian motion.[39] Since highly charged particles are characterized by reduced diffusion, the instrument detects them as larger than their geometrical size. In order to confirm that the particles did not undergo significant swelling at pH 10, the particles' diameter was also measured using reflection confocal microscopy, as described in the Methods section. This technique indeed did not show any significant difference in the particle size at pH 8 and 10 (Figure S5). We did not attempt atomic force microscope (AFM) measurements in solution since the size of the particles would be strongly affected by interactions of an AFM tip with the charged surface. In the effort to size the particles by yet another independent method, we imaged the pH 8 and pH 10 particles' suspensions using scanning electron microscopy in the environmental mode at room temperature. The particles' suspensions were placed on a porous support, and the images collected within a few minutes of achieving a vacuum of 0.6 mbar. At the time of taking images the solution was visibly evaporated; the average size as estimated by SEM was on average the same in both samples prepared at pH 8 and pH 10 (Figure S6).

As further evidence for the lack of particle swelling at pH 10, we sized the highly charged particles from a suspension in pH 8 after lowering it from its initially prepared pH of 10. Adjusting the pH from 10 to 8 reduced the effective size of the particles as measured by Zetasizer from 402 nm to 396 nm; thus a value that is close to 384 nm was obtained when the particles were placed from the stock solution directly into 0.1 M KCl, pH 8 (Figure S7). The magnitude and the shape of resistive pulses obtained using the same suspensions suggested that, indeed, the effective size of the particles was reduced when changing the pH from 10 to 8 (Figure S7). The recordings also indicated that some of the additional charges that the particles acquired at pH 10 due to deprotonation remained even after 2 h of incubation at pH 8. We do not yet have an explanation for this effect and will investigate it in the future.

The effect of enhanced current blockage caused by highly charged particles was further examined using particle suspensions prepared in different KCl concentrations. The uncharged 400 nm polystyrene spheres and weakly charged 410 nm carboxylated particles blocked the current to an extent that was only weakly dependent on the KCl concentration and pH (Figure 3). However, the current blockage caused by the highly charged particles was much larger in the more diluted KCl solution. In addition, increasing the salt concentration decreased the dependence of the pulse amplitude on pH.

We also verified that the effect of the increased resistive-pulse magnitude at pH 10 recorded for charged 400 nm particles could be observed for particles of different diameter. Figure S8 shows that charged 280 nm diameter particles exhibit similar behavior and produce larger current drop when passing through a pore at pH 10 compared to the recordings at pH 8.

According to the classical Coulter counter technique, due to the ohmic behavior of pores used for detection, the relative pulse amplitude $\Delta I/I$ remains constant under different applied voltages.[1−3] In spite of linear current−voltage curves of pores used in the experiments reported here (Figure S9), we noticed

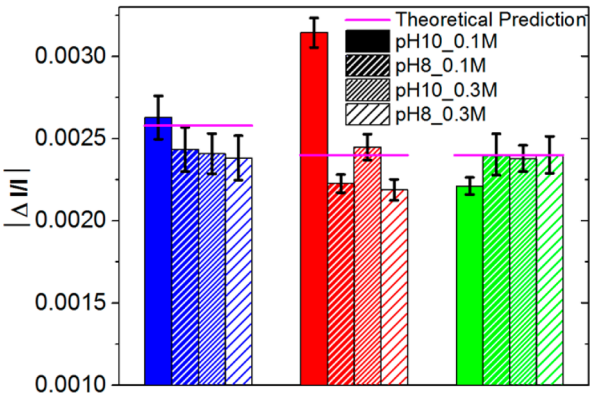

Figure 3. Average current blockage caused by charged 410 and 400 nm spheres, as well as neutral 400 nm diameter spheres under 0.4 V. The magenta lines are the theoretical predictions of $\Delta I/I$ based on the dimensions of particles and the pore.[2,3,6] This is the same PET pore as studied in Figures 1 and 2.

that the magnitude of $\Delta I/I$ for the highly charged particles increased with the increase of applied voltage until it reached a saturation value at ~1.5 V (Figure 4). It is important to note that an enhancement of the current blockage with voltage of one polarity has been recently observed with neutral and charged particles in conically shaped mesopores; for the opposite voltage polarity, an increase of voltage magnitude reduced the current blockage.[14] The voltage-induced modulations of $\Delta I/I$ in conical pores were however attributed to the pore shape; in a conical pore with surface charges, ionic concentrations and resistive-pulse amplitude are dependent on both the voltage magnitude and polarity.[13,15] Note that the effects presented here focus on large aspect ratio symmetric pores, which are characterized by voltage-independent ionic concentrations; thus the increase of $\Delta I/I$ with voltage has a different origin than in conically shaped pores. Moreover, the current blockages we analyze correspond to particles being inside the pore, and not the entrance/exit effects, responsible for the biphasic character of the pulses (current decrease followed by current increase above the baseline current).[13,28,29]

In order to understand the dependence of the resistive-pulse amplitude on the particle surface charge, we investigated in detail how the particle charge density in equilibrium, σ_p, depends on both solution pH and the density of functional groups, N_t, on the particle surface. To make the system numerically tractable, both the particle and pore diameter were scaled down by a factor of 10 compared to experimental values. As a result, particles with a radius of 20 nm (R_p) and a pore with an opening of 50 nm in radius (R_N) and 1100 nm in length (L_N) were considered. Note that the scale-down of the system in modeling under consideration will not change the qualitative results in the present study, which has been verified in Figures S10 and S11 of the Supporting Information. The functional carboxyl groups were assumed to be present either in protonated (uncharged) or in deprotonated (negatively charged) state.

Figure 5 presents σ_p as a function of solution pH for two values of N_t, 0.2 and 1.2 sites/nm^2, at the background KCl concentration C_{KCl} = 100 mM. The values of N_t were chosen to maximize the effect of the surface charge density on the particle transport and the magnitude of resistive pulses. The magnitude of σ_p was estimated based on the Poisson−Boltzmann model taking into account not only the surface chemistry reaction of

DOI: 10.1021/acsnano.6b03280
ACS Nano 2016, 10, 8413−8422

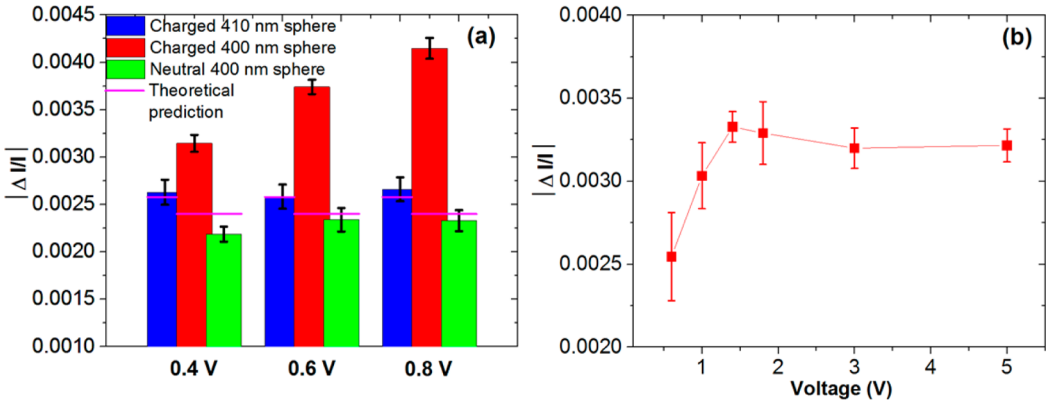

Figure 4. Normalized current blockage as a function of the applied voltage for two pores in 100 mM KCl, pH 10 solution. (a) Data for three types of particles, which passed through a PET pore with an opening diameter of 1550 nm. (b) Current blockage caused by translocations of the highly charged 400 nm diameter polystyrene particles through a single 1150 nm diameter PC pore; experiments at a wide range of voltages are shown. The magenta lines represent the theoretical predictions of $\Delta I/I$ based on the dimensions of particles and pores.[2,3,6] The theoretically predicted $\Delta I/I$ for the charged 400 nm particles in the PC pore is 0.001 73 (see Figure 2).

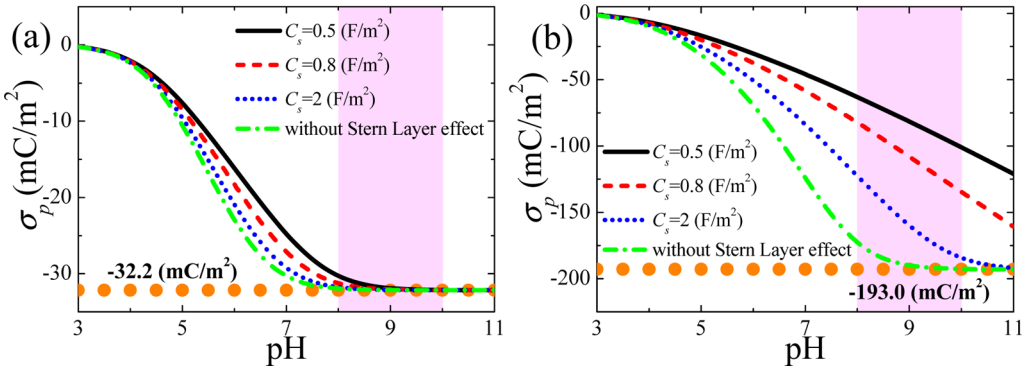

Figure 5. Variations of the surface charge density (σ_p) of carboxylated polystyrene particles with pH for various values of the surface capacitance of the Stern layer, C_s, for the surface density of carboxyl groups (sites) on the particle wall N_t = 0.2 (a) and 1.2 sites/nm^2 (b) when C_{KCl} = 100 mM, pK_a = 5.1, and R_p = 20 nm. The pink regions highlight the experimental conditions (pH 8 and 10). The discrete spheres denote the saturated values of σ_p when the carboxylated functional groups on particles are fully dissociated.

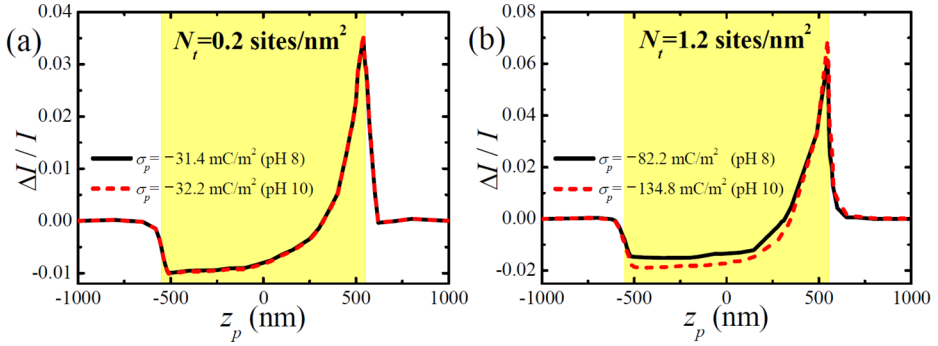

Figure 6. Numerical modeling of the normalized ion current blockage, $\Delta I/I$, as a function of the particle axial position, z_p, for various surface charge densities of a particle, σ_p. The values of σ_p adopted for solid and dashed lines in (a) are extracted from Figure 5a (N_t = 0.2 sites/nm^2) for pH 8 and 10, respectively, at C_s = 0.8 F/m^2; those in (b) are from Figure 5b (N_t = 1.2 sites/nm^2). Other simulation conditions include the following parameters: C_{KCl} = 100 mM, R_p = 20 nm, R_N = 50 nm, L_N = 1100 nm, the pore wall surface charge density σ_w = −30 mC/m^2, and V = 1 V. The yellow areas highlight the region where the particle is located in the pore interior.

carboxyl groups (~COOH ↔ COO$^-$ + H$^+$ with pK_a = 5.1)[40] but also the effect of the Stern layer, *via* the layer capacitance, C_s. Note that considering the Stern layer is crucial especially in the experimentally examined pH range of 8−10; calculating surface charge density without the Stern layer effects would render nearly no change of σ_p at high pH values. Three different values of C_s were considered (Figure 5). In general, with the decrease of the value of C_s (ranging typically from 0.15 to 2.9 F/m^2),[41] the effect of the Stern layer on the surface charge density becomes more significant. More details of modeling can be found in our recent work.[27]

Another surprising finding shown in Figure 5 is the effect of the density of the charged groups, N_t, on the character of the pH dependence of σ_p, especially in basic solutions. In the case

DOI: 10.1021/acsnano.6b03280
ACS Nano 2016, 10, 8413−8422

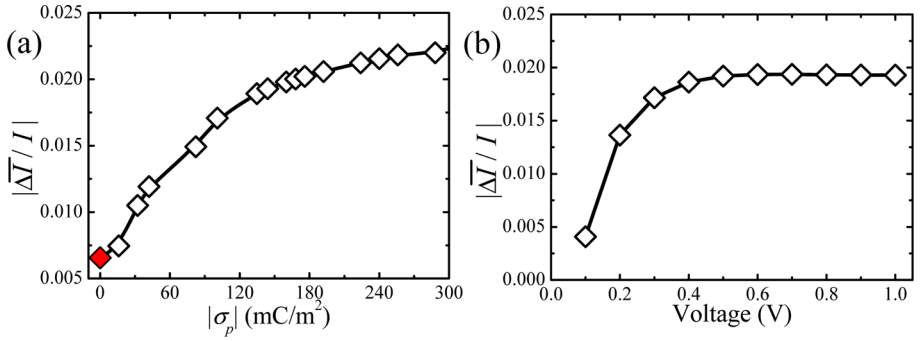

Figure 7. Dependence of the average value of absolute normalized current blockage, $|\overline{\Delta I}/I|$, on the magnitude of the surface charge density of a particle, $|\sigma_p|$, at V = 1 V (a) and on the applied voltage V (b) at σ_p = −134.8 mC/m^2. The red diamond in (a) highlights the result for a neutral particle. Other parameters are the same as those in Figure 6.

of the lower value of N_t = 0.2 sites/nm^2, the particle's surface charge density is only weakly sensitive to the variation of pH in the range examined experimentally (pH 8 to 10), independent of whether the Stern layer effect is considered or not (Figure 5a). On the other hand, if N_t is relatively large (1.2 sites/nm^2), the surface charge density of a particle for 8 ≤ pH ≤ 10 becomes high and visibly dependent on the value of C_s. In the limiting case of $C_s \rightarrow \infty$, *i.e.*, when the Stern layer is not taken into account, even in the case of high N_t, the pH dependence of the surface charge density for 8 ≤ pH ≤ 10 vanishes. This analysis highlights that neglecting the Stern layer effect could yield an incorrect estimation of the particle's surface charge density, particularly for particles with high densities of surface functional groups, N_t, and for pH ≫ pK_a.

For illustration, the particle's surface charge densities extracted from Figure 5a and b at C_s = 0.8 F/m^2 were subsequently used for the modeling of the electrokinetic translocation of single particles in a pore. The particle's surface charge densities were σ_p = −31.4 and −32.2 mC/m^2 (−82.2 and −134.8 mC/m^2) for pH 8 and 10 at N_t = 0.2 sites/nm^2 (1.2 sites/nm^2), C_{KCl} = 100 mM, respectively. The surface charge density of a pore was assumed as σ_w = −30 mC/m^2. Figure 6 depicts the numerical modeling results of the normalized current blockage, $\Delta I/I = (I - I_0)/I$, due to the translocation of particles with different values of σ_p, as mentioned above, through a pore at the applied voltage V = 1 V. Here, I_0 denotes the baseline ionic current of an empty pore, and the relationship of $\Delta I/I$ *versus* particle axial position, z_p, is shown. Figure 6 clearly indicates that the magnitude of ionic current blockage and σ_p depend highly on the density of functional groups, N_t. If the particle bears the lower density of carboxyl groups (*i.e.*, N_t = 0.2 sites/nm^2), changing the pH from 8 to 10 increases the effective surface charge density only by ∼0.1 mC/m^2 (from σ_p = −31.4 to −32.2 mC/m^2), resulting in similar current blockages at these two conditions (Figure 6a). By contrast, if the particle carries a higher surface site density of carboxyl groups (*i.e.*, N_t = 1.2 sites/nm^2), the magnitudes of σ_p for pH 8 and pH 10 are significantly different. As a result, both the magnitudes of current blockade and enhancement at the end of the pulse increase as the magnitude of the surface charge density of a particle increases.[22] The predicted pulses show excellent qualitative agreement with our experimental observations shown in Figures 1 and 2. Note that the predicted magnitude of the current increase accompanying particle exit is significantly higher than observed experimentally, which we think is related with scaling the experimental system down by a factor of 10. Ionic properties of a pore with an opening diameter of 100 nm will be affected by surface charge properties to a larger extent than a micrometer-sized pore; however qualitative conclusions are independent of the scaling (Figures S10 and S11). The goal of the modeling is however to provide an intuitive physical explanation of how surface charge density of particles can influence the magnitude of resistive pulses and not quantitative fitting of the experimental data.

In order to further unravel the influence of the magnitude of a particle's surface charge density, $|\sigma_p|$, and the applied voltage on ion current blockage in resistive-pulse experiments, average values of $|\overline{\Delta I}/I|$ for a wide range of $|\sigma_p|$ and applied voltages are shown in Figure 7. Here, $|\overline{\Delta I}/I|$ is calculated based on the average of five data points for axial positions −500 nm ≤ z_p ≤ − 100 nm. Figure 7a shows that the magnitude of $|\overline{\Delta I}/I|$ caused by a charged particle ($\sigma_p \neq 0$, open diamonds) is indeed higher than the current blockage caused by a neutral particle (σ_p = 0, red diamond) of the same diameter. In addition, the magnitude of $|\overline{\Delta I}/I|$ increases with $|\sigma_p|$ and gradually approaches a saturation value. $|\overline{\Delta I}/I|$ *versus* voltage also reaches a saturation, in accordance with experimental findings shown in Figure 4.

It is known that the current blockade caused by translocating particles arises mainly from the exclusion of an equivalent volume of salt solution by the particle, while the current enhancement stems from the enrichment of counterions carried by the charged particle into the pore.[11,12] The amplitude of the current blockade signal is used to measure the size of the passing objects; that is, a larger current blockage is recorded for larger particles.[1−3] However, our experimental and theoretical results demonstrate that the current blockage in a cylindrical pore can depend not only on the object size but also on the object's surface charge properties and even applied voltage. As mentioned above, this finding is unexpected because a particle with higher charge density should bring more counterions into the pore (see Figure S12 of the Supporting Information) and, therefore, yield less significant current blockade. Furthermore, in 100 mM KCl, the Debye length is orders of magnitude smaller than the pore radius, and thus the volume exclusion/physical blocking by the particle should indeed dominate the current blockade.

After careful analysis of local ionic concentrations and electric field in the pore with and without a particle, we concluded that an increase of the normalized current blockage with increasing a particle's surface charge density resulted from two effects: (a) a decrease in the magnitude of local electric field in the pore (see Tables S1 and S2 in the Supporting

DOI: 10.1021/acsnano.6b03280
ACS Nano 2016, 10, 8413−8422

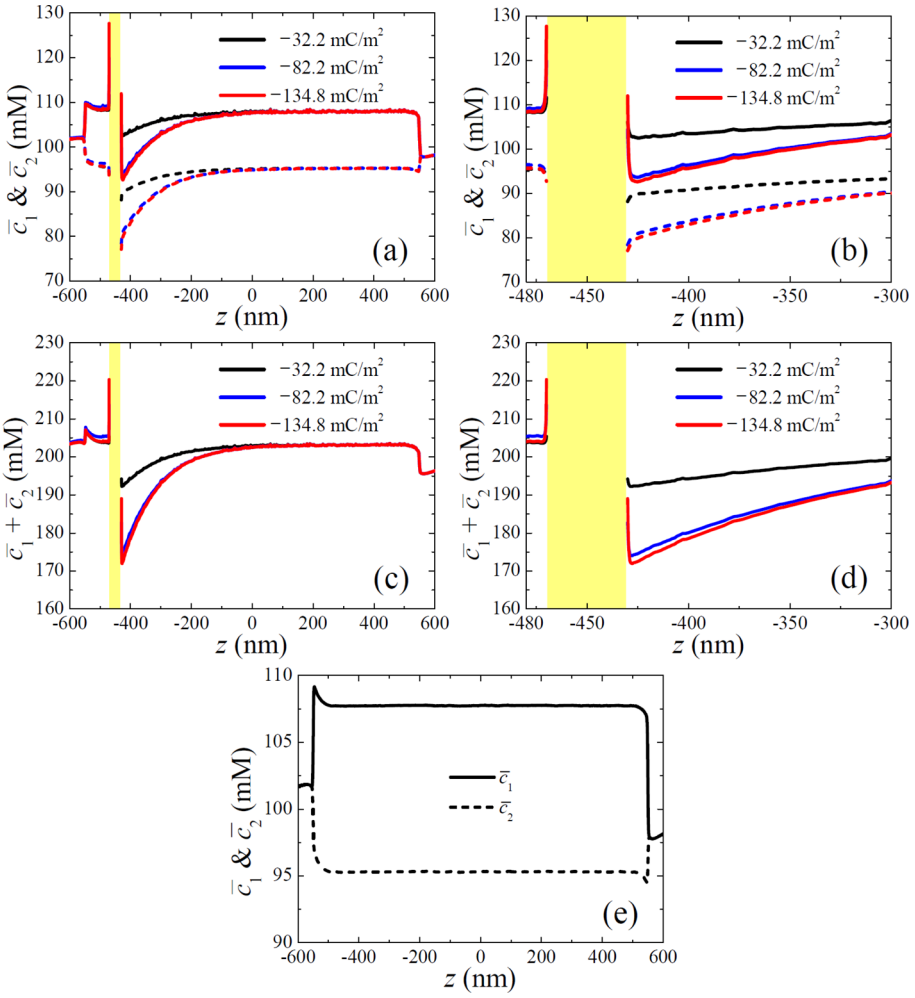

Figure 8. Axial variations of the cross-sectionally averaged concentrations of cations $\bar{c}_1$ (solid curves) and anions $\bar{c}_2$ (dashed curves) (a and b) and net ions $\bar{c}_1 + \bar{c}_2$ (c and d) for three magnitudes of σ_p. (b) and (d) denote, respectively, the magnified results of (a) and (c) with the emphasis of the region near the particle. (e) Corresponding results of $\bar{c}_1$ and $\bar{c}_2$ in the absence of a nanoparticle. The yellow regions in (a)−(d) highlight the region of a particle located at $z_p = -450$ nm. Other parameters are the same as those in Table S1.

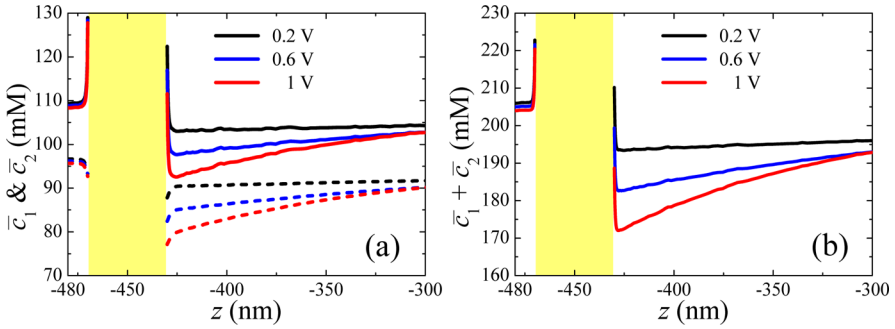

Figure 9. Magnified axial variations of the cross-sectionally averaged concentrations of cations $\bar{c}_1$ (solid curves) and anions $\bar{c}_2$ (dashed curves) (a) and net ions $\bar{c}_1 + \bar{c}_2$ (b) for three levels of the applied voltage. The yellow regions highlight the region of a particle located at $z_p = -450$ nm. Other parameters are the same as those in Table S2.

Information) and (b) concentration polarization in the vicinity of a translocating particle (Figures 8 and 9).

It is known that the local electric field within a pore will be significantly enhanced because of the larger difference of the linear size of a microscopic pore and that of a macroscopic reservoir. In the absence of charged particles (CPs), the electric field within a pore is primarily influenced by the charged pore,[42] while it will be influenced simultaneously by the charged particles and pore if CPs are present in the pore. The more significant squeeze effect by the charged particles and pore thus results in the more apparent percentage difference (PD) of the cross-section-averaged axial electric field between the results with and without a CP, defined by PD = $100\% \times |\bar{E}_z(\text{w/CP}) - \bar{E}_z(\text{w/o CP})|/|\bar{E}_z(\text{w/o CP})|$, shown in Table S1. When the particle bearing a higher surface charge density enters the pore, it results in a more significant decrease in the strength of the

DOI: 10.1021/acsnano.6b03280
ACS Nano 2016, 10, 8413−8422

local electric field and, therefore, a more significant decrease in the ionic current (more apparent current blockade). Similarly, we also verify in Table S2 in the Supporting Information that a higher applied voltage causes a more significant decrease in the local electric field in the pore when a highly charged particle is present, thus yielding a more significant current blockade.

We also found that electrokinetic passage of a particle through a pore modulates the concentration of both ions (cations and anions) in the vicinity of the particle, according to the mechanism of concentration polarization (Figures 8 and 9). As a result, a region with depleted ionic concentrations is formed in front of the passing particle, while a region with enhanced concentrations of ions is placed at the back of the particle (Figure 8). Moreover, the size of the depletion zone and the levels of ion concentrations are strongly voltage dependent, explaining our experimental result on the increase of $\Delta I/I$ with voltage (Figure 9).

Figure 10 summarizes our explanation of the increased amplitude of resistive pulses caused by highly charged particles.

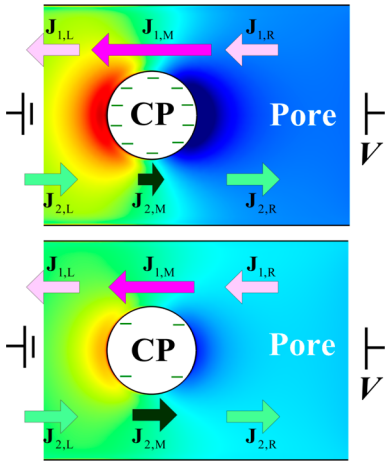

Figure 10. Schematic illustrations of the ion concentration polarization phenomenon near a charged particle (CP) passing through a pore. The upper and lower panels present cases with highly charged and weakly charged particles passing through a negatively charged pore. The left-hand side of the pore is grounded, while its right-hand side is at a positive potential V (>0). $J_{1,L}$, $J_{1,M}$, and $J_{1,R}$ ($J_{2,L}$, $J_{2,M}$, and $J_{2,R}$) denote the ionic fluxes of cations (anions) at the left-hand, middle, and right-hand sides of particle, respectively. Particles with higher surface charge density cause a more significant concentration polarization near the particle.

Due to the nearly insignificant Debye screening length in our system, the fluxes of cations and anions in the left-hand and right-hand sides of the pore are equal to each other but occur in opposite directions, yielding $|J_{1,L}| \approx |J_{2,L}| \approx |J_{1,R}| \approx |J_{2,R}|$. However, with a particle in the pore, a constriction zone with enhanced cation selectivity is present between the particle and the pore walls, yielding $J_{1,M} > J_{2,L}$. Consequently, two regions with depleted and enriched ionic concentrations are formed in the front and the back of the passing particle.[43] We postulate that the region with depleted ionic concentrations could dominate the ion current behavior and result in an increased blockade signal, $\Delta I/I$. Since more highly charged particles cause enhanced local ionic selectivity as well as stronger interactions between the charged particles and the pore, the extent of the depletion region in the pore increases accordingly, yielding an increased $\Delta I/I$. On the other hand, when the charged particles leave a pore, the ionic current behavior becomes dominated by the enriched region of ionic concentrations behind the particle, and a current enhancement is observed.

CONCLUSIONS

This article describes physical and chemical phenomena accompanying transport of charged mesospheres through single pores. Consequently, a zone with depleted ionic concentrations, formed in front of the passing particle, contributes to the recorded current blockage; the resistive-pulse amplitude is the measure of not only the object's volume but also the size of the depletion zone. This observation is surprising, because earlier experiments with nanopores and DNA molecules[10,11] as well as micropores and beads[13] indicated that highly charged objects could decrease the resistive-pulse amplitude. Concentration polarization across a translocating particle was hypothesized to explain experiments with translocating hydrogel particles,[17−19] but in this system the depletion zone was induced by the particle's intrinsic porosity and low density. The observation of concentration polarization accompanying translocation of hard spheres reported here points to the importance of considering local electric fields and ionic concentrations to correctly relate the pulse amplitude with the object size.

METHODS

Pore Preparation. Single pores in 12 μm thick polyethylene terephthalate and 30 μm thick polycarbonate films were prepared by the track-etching technique as reported before.[30] Wet chemical etching of the irradiated foils decreased the foil thickness by ~1 μm, and the pore lengths reported here are 11 and 29 μm, respectively. The foils were circular in shape and had a diameter of 3 cm. A single pore was positioned in the middle with a precision of ~1 mm. The pore-opening diameter was calculated from the pore resistance measured in 1 M KCl and assuming a cylindrical shape of the pore.

Particles. The particles used in the resistive-pulse experiments were purchased from Bangs Laboratories (Fisher, IN, USA). Carboxylated polystyrene particles with 410 and 400 nm diameters as well as unmodified thus uncharged 400 nm polystyrene particles were used in all measurements, with the exception of Figure S2, in which passage of a neutral poly(methyl methacrylate) particle is shown, and Figure S7, containing data with 280 nm carboxylated polystyrene particles; these are nominal diameters given by the manufacturer. The surface charge densities provided by the manufacturer should be used only in a comparative manner: the surface charge density of the 400 nm carboxylated particles was 3 times higher than the surface charge density of carboxylated 410 nm particles. Specifically, using the parking area of carboxyl groups as given by Bangs Laboratories, we calculated the density of carboxyl groups to be ~3.5, 10, and 3.2 per nm^2 for the 280, 400, and 410 nm particles, respectively. The high densities of the groups suggest that multiple carboxyl groups reside on polymer chains exposed to the solution. The diameter of all particles was measured using Zetasizer Nano ZS (Malvern Instruments, Westborough, MA, USA) in 100 mM KCl at pH 8 and pH 10. Measurements at higher salt concentration were not possible due to high conductivity of the solutions. The particles were also analyzed using a FEI Quanta 3D FEG Dual Beam (SEM/FIB).

Ion Current Recordings and Particle Detection. Resistive-pulse experiments were performed from suspensions prepared in 100 and 300 mM KCl with pH values ranging from 8 to 10, containing 0.1% (v/v) Tween 80. Suspensions containing both charged and uncharged particles were prepared and used in the resistive-pulse experiments; the concentration of all particles was ~10^9 particles/mL. Ion current measurements were performed with Axopatch 200B and 1322A Digidata (Molecular Devices, Inc.) using a sampling frequency of 20 kHz. The data were subjected to a low-pass Bessel filter of 1 kHz. Negatively charged particles translocated by electrophoresis and moved toward a positively biased electrode; neutral particles passed

DOI: 10.1021/acsnano.6b03280
ACS Nano 2016, 10, 8413−8422

through the pores by electroosmosis toward a negatively biased electrode.

Determination of Particle Size Using Reflection Confocal Microscopy. Suspended 400 nm highly charged particles in 100 mM KCl at pH 8 and 10 were measured using reflection microscopy. The immobile particles attached to the glass surface were found using an averaging filter. The images were measured using a 559 nm diode laser and with a 60× 1.2 NA objective offering a diffraction-limited point spread function of ∼280 nm. The images were analyzed using ImageJ to threshold the background using a Yen filter and later processed to measure the area of the detected particles with circularity in the range of 0.5 to 1. The particle radius was calculated and plotted as shown in Figure S5. Statistical analysis was calculated to find the p value using Student's t test.

Theoretical Modeling. The surface charge density of a carboxylated polystyrene particle under various solution pH's is determined by using the Poisson−Boltzmann model with simultaneously taking into account the surface interfacial reactions of dissociable carboxyl groups (∼COOH ↔ COO^- + H^+ at pK_a = 5.1)[40] and the Stern layer effect on the particle wall. The detailed solution procedure can be found in a recent study of Mei *et al.*[24] The electrokinetic translocation of a spherical particle through a cylindrical pore is modeled using the Poisson−Nernst−Planck equations in conjunction with the Navier−Stokes equation. The governing equations and associated boundary conditions (see details in the Supporting Information) are solved by COMSOL Multiphysics (version 4.3a), operated in a high-performance cluster. On the basis of the assumption of quasi-steady state, the ionic current change due to the passage of a charged particle through a pore under various conditions can be determined by a balance of the net forces, including electrical and hydrodynamic drag forces,[26] acting on a particle in the direction of an applied electric field. The finite element analysis based on the quasi-steady-state method using COMSOL has been verified to be sufficiently accurate and effective for similar electrokinetic DNA[44] and nanoparticle[45] transport problems, and a more detailed procedure can be found in the Supporting Information.

ASSOCIATED CONTENT

Supporting Information

The Supporting Information is available free of charge on the ACS Publications website at DOI: 10.1021/acsnano.6b03280.

Scheme of experimental setup, measurements of particle size by reflection confocal microscopy, as well as details of numerical modeling (PDF)

AUTHOR INFORMATION

Corresponding Authors

*E-mail (L.-H. Yeh): lhyeh@yuntech.edu.tw.
*E-mail (Z. S. Siwy): zsiwy@uci.edu.
*E-mail (J.-P. Hsu): jphsu@ntu.edu.tw.

Author Contributions

¶Y. Qiu and C.-Y. Lin contributed equally.

Notes

The authors declare no competing financial interest.

ACKNOWLEDGMENTS

Irradiation with swift heavy ions was performed at the GSI Helmholtzzentrum für Schwerionenforschung GmbH, Darmstadt, Germany. ESEM work was performed at the UC Irvine Materials Research Institute (IMRI), using instrumentation funded in part by the National Science Foundation Center for Chemistry at the Space-Time Limit (CHE-082913). We would like to thank Dr. Jian-Guo Zheng of UC Irvine's Laboratory for Electron and X-ray Instrumentation (LEXI) for guidance. This research was supported by the National Science Foundation (CHE 1306058). Y.Q. acknowledges financial support from the Scientific Research Foundation of Graduate School of Southeast University (YBPY 1504) and the China Scholarship Council (CSC 201406090034). L.H.Y. would like to express his sincere gratitude to the Ministry of Science and Technology, Taiwan (MOST 102-2221-E-224-052-MY3, 103-2221-E-224-039-MY3, and 105-2221-E-224-058-MY3), for its financial support.

REFERENCES

(1) Coulter, W. H. Means for Counting Particles Suspended in a Fluid. U.S. Pat. No. 2,656,508, 1953.
(2) DeBlois, R. W.; Bean, C. P.; Wesley, R. K. A. Electrokinetic Measurements with Submicron Particles and Pores by the Resistive Pulse Technique. *J. Colloid Interface Sci.* **1977**, *61*, 323−335.
(3) DeBlois, R. W.; Bean, C. P. Counting and Sizing of Submicron Particles by the Resistive Pulse Technique. *Rev. Sci. Instrum.* **1970**, *41*, 909−916.
(4) Berge, L. I.; Feder, J.; Jøssang, T. A Novel Method to Study Single-Particle Dynamics with Resistive Pulse Technique. *Rev. Sci. Instrum.* **1989**, *60*, 2756−2763.
(5) Luo, L.; German, S. R.; Lan, W.-J.; Holden, D. A.; Mega, T. L.; White, H. S. Resistive-Pulse Analysis of Nanoparticles. *Annu. Rev. Anal. Chem.* **2014**, *7*, 513−535.
(6) Henriquez, R. R.; Ito, T.; Sun, L.; Crooks, R. M. The Resurgence of Coulter Counting for Analyzing Nanoscale Objects. *Analyst* **2004**, *129*, 478−482.
(7) Bayley, H.; Martin, C. R. Resistive-Pulse Sensing − From Microbes to Molecules. *Chem. Rev.* **2000**, *100*, 2575−2594.
(8) Kasianowicz, J. J.; Brandin, E.; Branton, D.; Deamer, D. W. Characterization of Individual Polynucleotide Molecules Using a Membrane Channel. *Proc. Natl. Acad. Sci. U. S. A.* **1996**, *93*, 13770−13773.
(9) Venkatesan, B. M.; Bashir, R. Nanopore Sensors for Nucleic Acid Analysis. *Nat. Nanotechnol.* **2011**, *6*, 615−624.
(10) Chang, H.; Kosari, F.; Andreadakis, G.; Alam, M. A.; Vasmatzis, G.; Bashir, R. DNA-Mediated Fluctuations in Ion Current through Silicon Oxide Nanopore Channels. *Nano Lett.* **2004**, *4*, 1551−1556.
(11) Smeets, R. M. M.; Keyser, U. F.; Krapf, D.; Wu, M.-Y.; Dekker, N. H.; Dekker, C. Salt Dependence of Ion Transport and DNA Translocation through Solid-State Nanopores. *Nano Lett.* **2006**, *6*, 89−95.
(12) Howorka, S.; Siwy, Z. Nanopore Analytics: Sensing of Single Molecules. *Chem. Soc. Rev.* **2009**, *38*, 2360−2384.
(13) Lan, W.-J.; Kubeil, C.; Xiong, J.-W.; Bund, A.; White, H. S. Effect of Surface Charge on the Resistive Pulse Waveshape During Particle Translocation through Glass Nanopores. *J. Phys. Chem. C* **2014**, *118*, 2726−2734.
(14) Qiu, Y.; Vlassiouk, I.; Chen, Y.; Siwy, Z. S. Direction Dependence of Resistive-Pulse Amplitude in Conically Shaped Mesopores. *Anal. Chem.* **2016**, *88*, 4917−4925.
(15) Weatherall, E.; Willmott, G. R. Conductive and Biphasic Pulses in Tunable Resistive Pulse Sensing. *J. Phys. Chem. B* **2015**, *119*, 5328−5335.
(16) Kozak, D.; Anderson, W.; Vogel, R.; Chen, S.; Antaw, F.; Trau, M. Simultaneous Size and ζ-Potential Measurements of Individual Nanoparticles in Dispersion Using Size-Tunable Pore Sensors. *ACS Nano* **2012**, *6*, 6990−6997.
(17) Holden, D. A.; Hendrickson, G.; Lyon, L. A.; White, H. S. Resistive Pulse Analysis of Microgel Deformation During Nanopore Translocation. *J. Phys. Chem. C* **2011**, *115*, 2999−3004.
(18) Holden, D. A.; Hendrickson, G. R.; Lan, W.-J.; Lyon, L. A.; White, S. H. Electrical Signature of the Deformation and Dehydration of Microgels During Translocation Through Nanopores. *Soft Matter* **2011**, *7*, 8035−8040.
(19) Pevarnik, M.; Schiel, M.; Yoshimatsu, K.; Vlassiouk, I. V.; Kwon, J. S.; Shea, K. J.; Siwy, Z. S. Particle Deformation and Concentration

DOI: 10.1021/acsnano.6b03280
ACS Nano 2016, 10, 8413−8422

Polarization in Electroosmotic Transport of Hydrogels through Pores. *ACS Nano* **2013**, *7*, 3720−3728.
(20) Blundell, E. L. C. J.; Vogel, R.; Platt, M. Particle-by-Particle Charge Analysis of DNA-Modified Nanoparticles Using Tunable Resistive Pulse Sensing. *Langmuir* **2016**, *32*, 1082−1090.
(21) Park, S.-J.; Taton, T. A.; Mirkin, C. A. Array-Based Electrical Detection of DNA with Nanoparticle Probes. *Science* **2002**, *295*, 1503−1506.
(22) Qiu, Y.; Yang, C.; Hinkle, P.; Vlassiouk, I.; Siwy, Z. S. Anomalous Mobility of Highly Charged Particles in Pores. *Anal. Chem.* **2015**, *87*, 8517−8523.
(23) Manning, G. S. Counterion Binding in Polyelectrolyte Theory. *Acc. Chem. Res.* **1979**, *12*, 443−449.
(24) Dukhin, S. S. Non-Equilibrium Electric Surface Phenomena. *Adv. Colloid Interface Sci.* **1993**, *44*, 1−134.
(25) O'Brien, R. W.; White, L. R. Electrophoretic Mobility of a Spherical Colloidal Particle. *J. Chem. Soc., Faraday Trans. 2* **1978**, *74*, 1607−1626.
(26) Lu, Q.; Terray, A.; Collins, G. E.; Hart, S. J. Single Particle Analysis Using Fluidic, Optical and Electrophoretic Force Balance in a Microfluidic System. *Lab Chip* **2012**, *12*, 1128−1134.
(27) Mei, L.; Chou, T. H.; Cheng, Y. S.; Huang, M. J.; Yeh, L. H.; Qian, S. Electrophoresis of pH-Regulated Nanoparticles: Impact of the Stern layer. *Phys. Chem. Chem. Phys.* **2016**, *18*, 9927−9934.
(28) Menestrina, J.; Yang, C.; Schiel, M.; Vlassiouk, I.; Siwy, Z. S. Charged Particles Modulate Local Ionic Concentrations and Cause Formation of Positive Peaks in Resistive-Pulse-Based Detection. *J. Phys. Chem. C* **2014**, *118*, 2391−2398.
(29) Chen, K.; Shan, L.; He, S.; Hu, G.; Meng, Y.; Tian, Y. Biphasic Resistive Pulses and Ion Concentration Modulation During Particle Translocation Through Cylindrical Nanopores. *J. Phys. Chem. C* **2015**, *119*, 8329−8335.
(30) Fleischer, R. L.; Price, P. B.; Walker, R. M. *Nuclear Tracks in Solids: Principles and Applications*; University of California Press: Berkeley, CA, 1975.
(31) Pevarnik, M.; Healy, K.; Toimil-Molares, M. E.; Morrison, A.; Létant, S. E.; Siwy, Z. S. Polystyrene Particles Reveal Pore Substructure as They Translocate. *ACS Nano* **2012**, *6*, 7295−7302.
(32) Pevarnik, M.; Schiel, M.; Yoshimatsu, K.; Vlassiouk, I. V.; Kwon, J. S.; Shea, K. J.; Siwy, Z. S. Particle Deformation and Concentration Polarization in Electroosmotic Transport of Hydrogels Through Pores. *ACS Nano* **2013**, *7*, 3720−3728.
(33) Qiu, Y.; Hinkle, P.; Yang, C.; Bakker, H. E.; Schiel, M.; Wang, H.; Melnikov, D.; Gracheva, M.; Toimil-Molares, M. E.; Imhof, A.; Siwy, Z. S. Pores with Longitudinal Irregularities Distinguish Objects by Shape. *ACS Nano* **2015**, *9*, 4390−4397.
(34) Müller, S.; Schötz, C.; Picht, O.; Sigle, W.; Kopold, P.; Rauber, M.; Alber, I.; Neumann, R.; Toimil-Molares, M. E. Electrochemical Synthesis of $Bi_{1-x}Sb_x$ Nanowires with Simultaneous Control on Size, Composition, and Surface Roughness. *Cryst. Growth Des.* **2012**, *12*, 615−621.
(35) Wang, C.; Wang, L.; Zhu, X.; Wang, Y.; Xue, J. Low-Voltage Electroosmotic Pumps Fabricated from Track-Etched Polymer Membranes. *Lab Chip* **2012**, *12*, 1710−1716.
(36) Apel, P. Yu.; Blonskaya, I. V.; Dmitriev, S. N.; Orelovitch, O. K.; Sartowska, B. Structure of Polycarbonate Track-Etched Membranes: Origin of the 'Paradoxical' Pore Shape. *J. Membr. Sci.* **2006**, *282*, 393−400.
(37) Powell, M. R.; Cleary, L.; Daveport, M.; Shea, K. J.; Siwy, Z. S. Electric-Field-Induced Wetting and Dewetting in Single Hydrophobic Nanopores. *Nat. Nanotechnol.* **2011**, *6*, 798−802.
(38) Queasada-Pérez, M.; Callejas- Fernández, J.; Hidalgo-Alvarez, R. An Experimental Test of the Ion Condensation Theory for Spherical Particles. *J. Colloid Interface Sci.* **2001**, *233*, 280−285.
(39) Chow, R. S.; Takamura, K. Electrophoretic Mobilities of Bitumen and Conventional Crude-in-Water Emulsions Using the Laser Doppler Apparatus in the Presence of Multivalent Cations. *J. Colloid Interface Sci.* **1988**, *125*, 212−225.
(40) Subir, M.; Liu, J.; Eisenthal, K. B. Protonation at the Aqueous Interface of Polymer Nanoparticles with Second Harmonic Generation. *J. Phys. Chem. C* **2008**, *112*, 15809−15812.
(41) Ma, Y.; Yeh, L. H.; Lin, C. Y.; Mei, L. J.; Qian, S. Z. pH-Regulated Ionic Conductance in a Nanochannel with Overlapped Electric Double Layers. *Anal. Chem.* **2015**, *87*, 4508−4514.
(42) Yeh, L. H.; Zhang, M.; Hu, N.; Joo, S. W.; Qian, S.; Hsu, J. P. Electrokinetic Ion and Fluid Transport in Nanopores Functionalized with Polyelectrolyte Brushes. *Nanoscale* **2012**, *4*, 5169−5177.
(43) Yeh, L. H.; Zhang, M.; Qian, S.; Hsu, J. P.; Tseng, S. Ion Concentration Polarization in Polyelectrolyte-Modified Nanopores. *J. Phys. Chem. C* **2012**, *116*, 8672−8677.
(44) Yeh, L. H.; Zhang, M.; Qian, S.; Hsu, J. P. Regulating DNA Translocation through Functionalized Soft Nanopores. *Nanoscale* **2012**, *4*, 2685−2693.
(45) Yeh, L. H.; Zhang, M. K.; Joo, S. W.; Qian, S.; Hsu, J. P. Controlling pH-Regulated Bionanoparticles Translocation through Nanopores with Polyelectrolyte Brushes. *Anal. Chem.* **2012**, *84*, 9615−9622.

DOI: 10.1021/acsnano.6b03280
ACS Nano 2016, 10, 8413−8422